Evidence for phonon-like charge and spin fluctuations from an analysis of angle-resolved photoemission spectra of $La_{2-x}Sr_xCuO_4$ superconductors

G. Mazza,[1,2] M. Grilli,[2,3] C. Di Castro,[2,3] and S. Caprara[2,3]

[1]*International School for Advanced Studies (SISSA), Via Bonomea 265, 34136 Trieste, Italy*

[2]*CNISM and Dipartimento di Fisica, Università di Roma "La Sapienza", Piazzale Aldo Moro 5, I-00185 Roma, Italy*

[3]*Consiglio Nazionale delle Ricerche, Istituto dei Sistemi Complessi, via dei Taurini, I-00185 Roma, Italy*

(Received 15 June 2012; revised manuscript received 7 January 2013; published 23 January 2013)

In high temperature superconductors we provide evidence of spin and mixed phonon-charge collective modes as mediators of the effective electron-electron interaction and suggestive of a charge and spin density wave instability competing with superconductivity. Indeed, we show that the so-called kinks and waterfalls observed in angle-resolved photoemission spectra of $La_{2-x}Sr_xCuO_4$, a prototypical high-T_c superconducting cuprate, are due to the coupling of quasiparticles with two distinct nearly critical collective modes with finite characteristic wave vectors, typical of charge and spin fluctuations. The simultaneous presence of these two modes reconciles the long standing dichotomy whether kinks are due to phonons or spin waves.

DOI: 10.1103/PhysRevB.87.014511 PACS number(s): 74.25.Jb, 74.20.−z, 74.72.−h, 79.60.−i

I. INTRODUCTION

The metallic phase of high-T_c superconducting cuprates evolves with changing the temperature T and the doping x. Around optimal doping $x \approx x_{\rm opt}$ (where the maximum superconducting critical temperature T_c is achieved) and for $T > T_c$, the metallic phase seems to be ruled by the temperature as the only relevant energy scale, a typical signature of quantum criticality. In underdoped samples, with $x < x_{\rm opt}$, a pseudogap opens around the Fermi energy below a doping-dependent crossover temperature $T^*(x)$. Whether this is accompanied by the onset of some sort of ordering is still a matter of debate. Nonetheless, models with nearly critical collective modes coupled to fermion quasiparticles may not only explain the anomalous metallic phase,[1–3] but also provide candidate mediators of a retarded pairing interaction (the so-called *glue*),[4–6] alternative to phonons in ordinary superconductors, and are therefore actively investigated.

Various proposals for sources of nearly critical collective modes include the antiferromagnetic phase at $x \approx 0$ (Ref. 7), time-reversal-breaking plaquette currents,[8] order parameters with exotic wave symmetry,[9–11] or charge-density-wave/stripe ordering proposed a longtime ago[12–14] and recently observed in x-ray experiments.[15,16] It is therefore crucial to identify the spectroscopic signatures of collective modes to ascertain their nature and to infer the associated underlying order. In this regard, the recent observation of *two* distinct collective modes contributing to the electron-electron effective interaction is of obvious relevance and it has attracted increasing attention.[17–19] The occurrence of two collective modes, both having *finite* and quite different characteristic wave vectors, is also the key point allowing the authors of Ref. 17 to separate and distinguish the contributions of each mode to the Raman spectra of $La_{2-x}Sr_xCuO_4$ (LSCO) in the various symmetry channels (as experimentally obtained by choosing the polarization of the ingoing and outgoing photons). This possibility is absent in optical experiments where, however, the presence of two collective modes has also been inferred in $Bi_2Sr_2CaCu_2O_8$ (BSCCO).[18,19]

The analysis of the Raman spectra of LSCO, carried out in Ref. 17 in the doping range $x = 0.15$–0.26 and for various temperatures, showed that one collective mode is essentially propagating and centered at typical phonon frequencies, and is associated with charge fluctuations strongly mixed with the lattice degrees of freedom. The second collective mode, more diffusive and extending to higher energies, is associated with spin fluctuations peaked near the wave vector of antiferromagnetic order. The behavior of the characteristic low-energy scale of the two collective modes suggests that a quantum critical point occurs at $x_{QCP} \approx 0.19$ (Refs. 12,20–22), associated to a phase with charge and spin modulation, setting via a harmonic incommensurate charge-density wave at $T \approx T^*(x)$ (Refs. 12,23,24). Remarkably, the strengths of the two collective modes have an opposite doping dependence (see Fig. 5 in Ref. 17): The strength of the spin collective mode decreases with increasing x and almost vanishes in the most overdoped sample ($x = 0.26$), whereas the strength of the charge collective mode increases with increasing x and tends to saturate in the overdoped regime. The value $x \approx 0.19$ marks the boundary between the charge- and spin-dominated regions at larger and smaller x, respectively. At low doping, spin fluctuations are naturally enhanced by incipient antiferromagnetism.

In this work, we consider the anomalies observed in the single-electron spectra by angle-resolved photoemission spectroscopy (ARPES) in cuprates, namely the so-called *kinks* and *waterfalls*:[25] The former are sudden changes in the quasiparticle velocity occurring at different binding energies in different regions of the Brillouin zone (BZ) and the latter are nearly vertical drops of the quasiparticle dispersions at high/moderate binding energies.[26,27] We show that in LSCO these anomalies are explained in terms of *both* charge and spin collective modes on the verge of an instability toward a phase with charge and spin modulation. The kinks gave rise to the long-standing phonon-vs-spin controversy because they have been attributed to a phonon with a near frequency[28,29] or, alternatively, to spin fluctuations in $YBa_2Cu_3O_{7-x}$ (YBCO),[30] and BSCCO.[31] The presence of both charge (mixed with phonons) and spin collective modes as sources of quasiparticle scattering, at least in LSCO, now provides a bridge for this dichotomy.

The scheme of the paper is as follows. In Sec. II we present the model, while in Sec. III we describe our ARPES perturbative analysis and we present the results. These are then discussed in Sec. IV, where we also draw our conclusions.

II. MODEL

Here we analyze the implications of the *same* collective modes, as derived from Raman experiments, on quasiparticle spectra. In our phenomenological model, similarly to the electron-phonon coupling, quasiparticles are coupled to these collective modes through dimensional coupling constants g_λ yielding the Hamiltonian

$$\mathcal{H} = \sum_{\mathbf{k},\sigma} \epsilon_{\mathbf{k}} c^\dagger_{\mathbf{k}\sigma} c_{\mathbf{k}\sigma} + \sum_{\mathbf{k},\mathbf{q},\alpha,\beta} \sum_i g_i c^\dagger_{\mathbf{k}+\mathbf{q}\alpha} c_{\mathbf{k}\beta} \tau^i_{\alpha\beta} \Phi^i_{-\mathbf{q}},$$

where the $c^\dagger_{\mathbf{k}\sigma}$ ($c_{\mathbf{k}\sigma}$) creates (annihilates) a fermionic quasiparticle of momentum $\mathbf{k}$ and spin projection σ. We adopt for the fermion quasiparticles on the CuO_2 planes of LSCO a tight-binding dispersion law including nearest ($t = 400$ meV) and next-to-nearest ($t' = -0.21t$) neighbor hopping terms, $\epsilon_{\mathbf{k}} = -2t[\cos(ak_x) + \cos(ak_y)] - 4t' \cos(ak_x)\cos(ak_y) - \mu$, where μ is the chemical potential and a is the spacing of the two-dimensional square lattice describing the CuO_2 planes of cuprates, henceforth taken as unit length.

The bosonic fields Φ^i represent the charge ($i = 0$) or the spin ($i = 1,2,3$) densities, τ^0 is the 2×2 identity matrix in spin space, and τ^1,τ^2,τ^3 are the Pauli matrices. In the following, since we only consider isotropic spin in the paramagnetic state, we consider a single spin component and englobe the spin multiplicity factor in the coupling constant (see, e.g., Ref. 32). The label $\lambda = C,S$ marks hereafter the charge and spin collective mode, respectively. According to this notation, the couplings with the charge and spin collective mode are indicated with g_C and g_S.

We assume that these bosonic (collective) degrees of freedom are near an instability and their propagator takes the standard Gaussian form, valid within both the classical and quantum Landau-Wilson approach, and already adopted for models of fermionic quasiparticles coupled to nearly critical charge[12] and spin[7,33] collective modes in the cuprates

$$\mathcal{D}_\lambda(\mathbf{q},\omega_n) = -\frac{1}{\Upsilon_\lambda(\mathbf{q}) + |\omega_n| + \omega_n^2/\overline{\Omega}_\lambda}, \qquad (1)$$

where ω_n is a bosonic Matsubara frequency and $\Upsilon_\lambda(\mathbf{q}) = m_\lambda + \nu_\lambda \eta_\lambda(\mathbf{q})$, with $\eta_\lambda(\mathbf{q}) = 2 - \cos[(q_x - Q_{\lambda,x})a] - \cos[(q_y - Q_{\lambda,y})a]$, describes the dispersion of a collective mode, with the periodicity of the lattice. m_λ is proportional to the inverse squared correlation length ξ_λ^{-2}, and ν_λ sets the curvature at the bottom of the collective mode dispersion law. The propagator (1) is peaked at a characteristic wave vector $\mathbf{Q}_\lambda$, has a diffusive character at low energy, and becomes more propagating above the energy scale $\overline{\Omega}_\lambda$. The dispersive region of the collective mode is limited in energy by a cutoff Λ_λ, setting a momentum cutoff $|\overline{\mathbf{q}}_\lambda| \approx (\Lambda_\lambda/\nu_\lambda)^{1/2}$. Indeed microscopic calculations based on the Hubbard-Holstein model[34] show that the charge collective mode essentially has a flattish phonon dispersion $\sim\omega_0$, which, near the charge instability, is substantially softened in a limited momentum region around $\mathbf{Q}_C$. The parameter $\overline{\mathbf{q}}_C$ sets the width of this dispersive region, where a parabolic dispersion in the poles of Eq. (1) extends from the energy scale m_C, to $\sqrt{\overline{\Omega}_C \Lambda_C}$. We assume that a similar momentum cutoff is present for the spin collective mode. The dynamics of the mixed phonon-charge collective mode within the Hubbard-Holstein model is a result of the interplay of the dynamics of the phonon and of the dynamical dependence of the electron screening (the Lindhard function). As a result, electron and phonon energy scales are mixed and one can show[3] that $\overline{\Omega}_C \approx \omega_0^2/t$ and $\Lambda_C \approx t$, yielding $\sqrt{\overline{\Omega}_C \Lambda_C} \approx \omega_0$. Therefore, the microscopic calculations of the authors of Refs. 3 and 34 support the result of the authors of Ref. 17, where the charge collective mode needed to describe the Raman spectra of LSCO is indeed found to be peaked at a typical phonon frequency.

TABLE I. Parameters of the charge and spin collective modes. m, Λ, $\overline{\Omega}$, and κ are extracted from Raman data (Ref. 17) at $T \approx 40$K. $\overline{\mathbf{q}}$ and $\mathcal{Q}$ are adjusted to fit ARPES spectra. The value of $\nu = \Lambda/\overline{\mathbf{q}}^2$ is also reported.

Charge							
x	m (meV)	Λ (meV)	$\overline{\Omega}$ (meV)	κ	$\overline{\mathbf{q}}$	ν (meV)	$\mathcal{Q}$
0.15	2.5	248.0	25.0	5.5	0.9	300.0	0.6
0.17	4.35	248.0	25.0	8.0	0.9	300.0	0.6
0.20	8.7	310.0	25.0	11.7	1.0	300.0	0.5
0.25	9.9	186.0	41.3	13.7	0.9	240.0	0.5
0.26	7.55	300.0	41.3	17.5	1.0	280.0	0.55
Spin							
x	m (meV)	Λ (meV)	$\overline{\Omega}$ (meV)	κ	$\overline{\mathbf{q}}$	ν (meV)	$\mathcal{Q}$
0.15	0.62	86.8	248.0	4.35	0.57	260.0	0.75
0.17	0.62	74.4	310.0	4.5	0.6	200.0	0.6
0.20	0.74	86.8	496.0	1.4	0.57	270.0	0.95
0.25	1.25	62.0	496.0	0.26	0.5	240.0	1.0
0.26	1.5	49.6	155.0	0.40	0.42	280.0	0.85

The values of the characteristic wave vectors are extracted from neutron scattering experiments on LSCO. The value of the incommensurability of the spin modulation saturates for $x > 1/8$ (Ref. 35), where the characteristic wave vectors of spin fluctuations are $\mathbf{Q}_S = \pi(1 \pm \frac{1}{4},1),\pi(1,1 \pm \frac{1}{4})$. The value of the incommensurability of the charge modulation is directly measured at $x = 1/8$ (Refs. 36 and 37), where it turns out to be twice as large as the value of the incommensurability of spin fluctuations, consistently with a stripe-like arrangement of segregated charges, and corresponds to characteristic wave vectors $\mathbf{Q}_C = \pi(\pm\frac{1}{2},0),\pi(0,\pm\frac{1}{2})$.

The analysis of Raman data on LSCO[17] yielded the doping evolutions of the collective mode parameters m, Λ, $\overline{\Omega}$, and $\kappa \equiv g^2/t\nu$, reported in Table I, which will be used to obtain the results shown in Figs. 2 and 4. However, it should be borne in mind that the Raman response is a momentum integrated quantity, so that the precise $\mathbf{q}$ dependence of the collective-mode-mediated effective interaction, and therefore the value of $\overline{\mathbf{q}}$, is not fully constrained. We adjust $\overline{\mathbf{q}}$ as a fitting parameter, which in turn fixes $\nu = \Lambda/\overline{\mathbf{q}}^2$ and $g = \sqrt{\kappa t \nu}$. The values of these parameters are also reported in Table I.

III. ARPES SPECTRA

The effect of collective modes on quasiparticle spectra is captured by computing the lowest-order quasiparticle self-energy reported in Fig. 1, $\Sigma(\mathbf{k},\omega) = \Sigma_C(\mathbf{k},\omega) + \Sigma_S(\mathbf{k},\omega)$, and the spectral density

$$A(\mathbf{k},\omega) = \frac{1}{\pi} \frac{|\mathrm{Im}\Sigma(\mathbf{k},\omega)|}{[\omega - \epsilon_{\mathbf{k}} - \mathrm{Re}\Sigma(\mathbf{k},\omega)]^2 + [\mathrm{Im}\Sigma(\mathbf{k},\omega)]^2}.$$

The imaginary part of the self-energy is

$$\mathrm{Im}\Sigma_\lambda(\mathbf{k},\omega) = g_\lambda^2 \int_{BZ} \frac{d^2\mathbf{q}}{(2\pi)^2}\, \gamma_\lambda(\mathbf{q}) \times \frac{(\omega - \epsilon_{\mathbf{k}-\mathbf{q}})[f_+(\epsilon_{\mathbf{k}-\mathbf{q}}) + f_-(\epsilon_{\mathbf{k}-\mathbf{q}} - \omega)]}{[\Upsilon_\lambda(\mathbf{q} - \mathbf{Q}_\lambda) - (\omega - \epsilon_{\mathbf{k}-\mathbf{q}})^2/\overline{\Omega}_\lambda]^2 + (\omega - \epsilon_{\mathbf{k}-\mathbf{q}})^2}, \quad (2)$$

where a sum over the equivalent wave vectors $\mathbf{Q}_\lambda$ is understood, $f_\pm(\omega) = 1/(e^{\omega/T} \pm 1)$, and the smooth cutoff function $\gamma_\lambda(\mathbf{q}) = \exp[-\eta_\lambda(\mathbf{q})/{\mathcal{Q}_\lambda}^2]$ accounts for the suppression of the coupling between the collective modes and quasiparticles away from $\mathbf{Q}_\lambda$. The range of variation of the self-energy and of the vertex in momentum space is expected to be of the same order, i.e., $\mathcal{Q}_\lambda \approx |\overline{\mathbf{q}}_\lambda|$, as it is confirmed by the values obtained fitting the ARPES spectra, reported in Table I. For any given $\mathbf{k}$ and ω, we numerically integrate Eq. (2) and obtain $\mathrm{Re}\Sigma$ via the Kramers-Kronig transformation. The chemical potential μ is fixed imposing that

$$2\int_{BZ} \frac{d^2\mathbf{k}}{(2\pi)^2} \int_{-\infty}^{+\infty} d\omega\, A(\mathbf{k},\omega) f_+(\omega) = 1 - x.$$

We calculate the ARPES intensity convoluting $A(\mathbf{k},\omega)$ with a Gaussian of width $\approx$10 meV, mimicking the energy resolution, and considering only the occupied states.

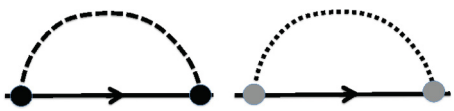

FIG. 1. Self-energy diagrams. The solid line is the bare quasiparticle propagator, the dashed (dotted) lines represent the charge (spin) collective mode propagators, Eq. (1), with $\lambda = C(S)$. The black and gray dots represent the couplings of quasiparticles with charge and spin collective modes g_C and g_S, respectively.

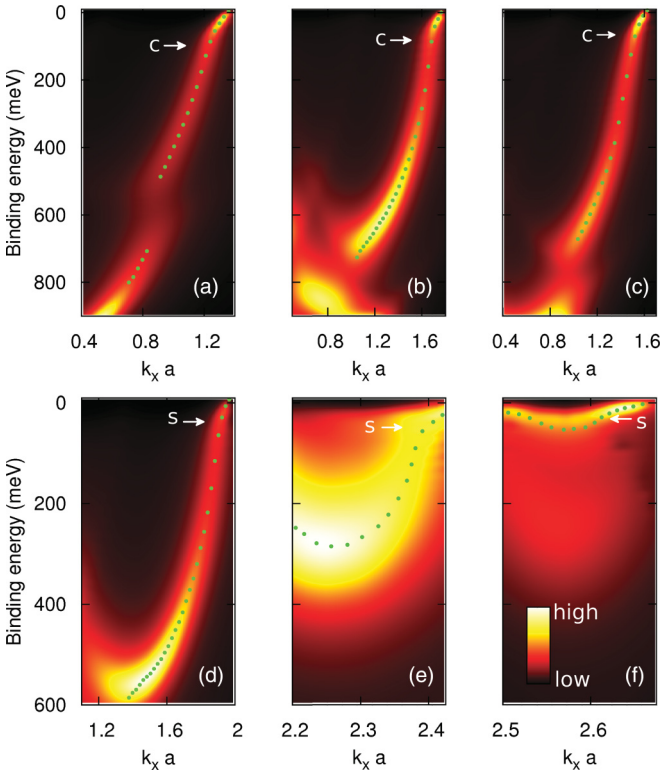

FIG. 2. (Color online) Spectral density along the cuts of the BZ reported in Fig. 3 for $x = 0.15$ and $T = 40$ K. Dots represent the maxima of the MDCs. The arrows mark the positions of the kinks and are labeled according to the collective mode which gives the dominant contribution to the kink (see text).

In Fig. 2, we report the spectra along the cuts A through F of Fig. 3, for $x = 0.15$ and $T = 40$ K. We track the quasiparticle dispersions (dots) as the maxima of the momentum distribution curves (MDCs). The condition of quasicriticality (small m_λ) and the finite characteristic wave vectors $\mathbf{Q}_\lambda$ render the scattering most relevant when the quasiparticle momenta $\mathbf{k}$ satisfy the *hot line* condition $\epsilon_{\mathbf{k}} = \epsilon_{\mathbf{k}\pm\mathbf{Q}_\lambda}$, identifying the points at the same energy on the quasiparticle bands, connected by $\mathbf{Q}_\lambda$. We report in Fig. 3 the hot lines for charge [(red) dashed lines] and spin [(blue) solid lines] collective modes. These lines intersect the Fermi surface at the so-called *hot spots*. Away from the hot lines, the scattering in Eq. (2) is not dominated by the low-energy collective mode spectrum, and is rather mediated by the whole dynamical range of the order of $\sqrt{\overline{\Omega}\Lambda}$. This energy scale determines the binding energy of the kinks ($\lesssim$70 meV) appearing in Fig. 2. On the other hand, the strong *quasistatic* scattering near the hot lines, reminiscent of the Bragg scattering occurring when some order sets in with finite $\mathbf{Q}_\lambda$ (Refs. 38 and 39), gives rise to the waterfall features at high binding energy in Fig. 2. An explanation of the waterfalls in terms of an electronic (spin) generated self-energy was already

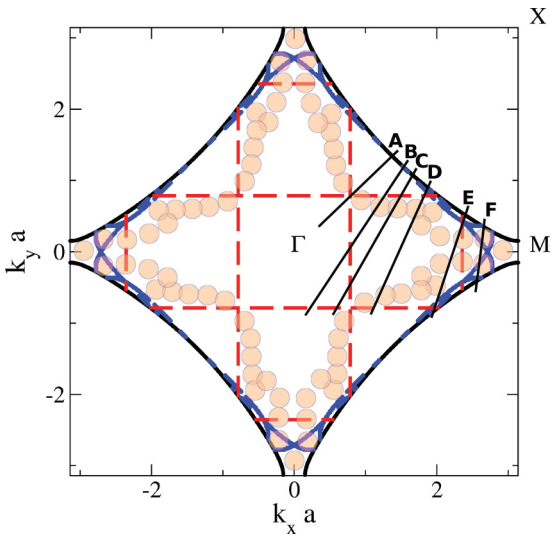

FIG. 3. (Color online) Fermi surface of LSCO at $x = 0.15$ (black solid line). The dashed (red) and solid (blue) lines mark the C and S hot lines, respectively. The shaded circles mark the loci of the waterfalls (from Ref. 27). The spectra in Fig. 2 are calculated along the cuts A to F.

proposed in Refs. 40–42. In these cases, however, only one mode was considered and the loci of the momenta where the waterfalls occur were not detailed. Moreover, in contrast with our results, in the absence of a hot-line condition, to obtain high-energy waterfalls as a kink due to quasiparticles scattered by a collective mode, a correspondingly high-energy mode is needed.[40–42]

A. The "waterfalls"

We obtain waterfalls that compare fairly well with the experiments,[25–27] although our perturbative scheme underestimates their binding energy and broadening. In particular, our hot lines (see Fig. 3) reproduce the loci of the BZ where the waterfalls are observed[27] (the shaded circles reported in Fig. 3). The waterfalls along the cuts Athrough C (at energies ≈600, ≈300, and ≈250 meV, respectively) correspond to the nearly cross-shaped accumulation of the loci well inside the BZ in Fig. 3, which in our scheme (red dashed lines) are due to charge incipient order. This incipient order also produces additional waterfalls along a square contour around the Γ point of the BZ. These are visible in panels B and C of Fig. 2, at ≈700–800 meV. Their presence cannot be ascertained in Ref. 27, where the data at higher binding energy are not reported. A reanalysis of the data is required to check whether hints of these additional waterfalls are visible despite the width of the spectra and the nearby presence of the oxygen-like bands.[43] On the other hand, both the scatterings mediated by charge and spin fluctuations are responsible for the dense occurrence of hot lines near the M points (as visible along the cuts D through F of Fig. 3). However, as it is clear from panels D through F in Fig. 2, the waterfalls are shifted to lower binding energy in this region of the BZ and merge with the kinks. Moreover, approaching the hot spots, the waterfall evolves into a rounding of the quasiparticle dispersions, with a spectral intensity vanishing as $\sqrt{\omega}$ (Refs. 7,32 and 44). This square root behavior is a signature of the violation of the Fermi liquid behavior near the hot spots due to an incipient criticality characterized by finite ordering wave vectors. The corresponding rounding of the spectra is reminiscent of the additional low-energy kinks observed in BSCCO,[45,46] but not in LSCO, possibly due to a lower resolution.

B. The "kinks"

The binding energy of the kinks depends on the collective mode dispersion and on the position of the cut with respect to the hot lines, which controls the above-mentioned merging with the waterfalls. In the nodal (ΓX) direction (cut A in Fig. 2), the kink is well separated from the waterfall and is closely inspected in Fig. 4(a). Here, we consider the separate contribution of charge [(red) squares] and spin [(green) triangles] collective modes to the kink, as well as the combined effect of both collective modes [(blue) circles]. The binding energy of the kink [marked by a blue arrow in Fig. 4(a)] evidently coincides with the characteristic energy scale of the charge collective mode [marked by a red arrow, see also the arrows marked by the label C in Fig. 2 (A–C)], at ≈60–70 meV, in good agreement with the experimental dispersion for LSCO at the same doping and temperature.[47] From the values of $\overline{\Omega}_C$ reported in Table I, we infer that the charge collective mode has a markedly propagating character. This makes its contribution to the kink rather sharp. This is consistent, with the aforementioned microscopic calculations of the authors of Ref. 34, showing that the charge collective mode has a flattish phonon dispersion $\sim\omega_0$, which, near the charge instability, is substantially softened in a limited momentum region of momentum space around the characteristic wave vector $\mathbf{Q}_C$.

Thus, the charge collective mode has a marked phonon character away from the hot lines.[32,34] We also emphasize that the characteristic energy of the charge collective mode

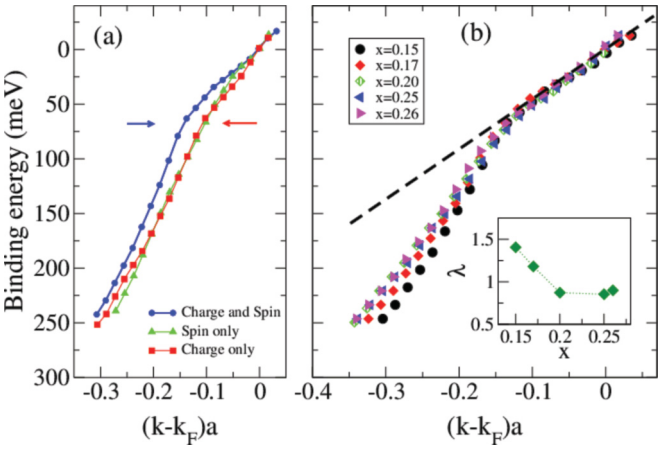

FIG. 4. (Color online) (a) Quasiparticle dispersion along the ΓX direction for LSCO at $x = 0.15$ and $T = 40$ K in the presence of both C and S collective modes [solid (blue) circles] and for C [(red) squares] or S [(green) triangles] only. (b) Quasiparticle dispersion along the ΓX direction for LSCO at various values of doping. Both C and S collective modes are considered, $T = 40$ K. The dashed straight lines marks the low-energy dispersion. Inset: Doping evolution of $\lambda \equiv (v_{HE}/v_F) - 1$ (see text).

is extracted from Raman experiments (Table I) and is not adjusted here by introducing additional collective modes with suitably chosen phonon frequencies. On the other hand, the more diffusive spin collective mode does not fix an energy scale and rather renormalizes the quasiparticle dispersion over a broader energy range, affecting the quasiparticle velocities far from the kink and making the kink more pronounced. Thus, both the charge and spin collective modes must be simultaneously taken into account to reproduce the observed behavior of the kink.

When the cut moves to the region where the charge hot line approaches the Fermi surface (cuts B through D), thus giving rise to the hot spots, the kink moves from $\sqrt{\bar{\Omega}_C \Lambda_C} \sim 70$ meV to lower binding energies. This shift entails an increasing interplay with the spin collective mode. Along the cuts E to F, the kinks strongly interfere with the waterfalls, producing mixed structures, as mentioned above. Since the charge and spin hot lines are intricate, it is difficult to distinguish the role of the two collective modes in determining the mixed kink-waterfall structures in this region of the BZ. Nonetheless, by switching on and off the couplings with the charge and spin collective mode, we can state that the spin collective mode plays the major role in determining the kinks and mixed kink-waterfall features in cuts D through F (the arrows marked by an S in Fig. 2).

C. Doping evolution of the kink

The analysis of Raman spectra shows that the interaction mechanism switches from spin to charge collective mode with increasing doping.[17] This characterizes the doping evolution of the quasiparticle dispersion in the range $x = 0.15$–0.26 (Ref. 47). In Fig. 4(b), one sees that the spin-vs.-charge switching produces no appreciable effect on the low-energy dispersion, which is determined cooperatively by the two collective modes, so that the initial slope remains quite constant in the considered doping range [the dashed line in Fig. 4(b)]. On the other hand, in the high-energy dispersion, most of the effect of the charge collective mode, peaked at a phonon frequency, is exhausted and the variation of the slope is controlled by the much broader spin collective mode. The dispersion becomes less steep with increasing doping, so that the high-energy quasiparticle velocity decreases. This is clearly observed looking at the inset in Fig. 4(b), where the parameter $\lambda \equiv (v_{HE}/v_F) - 1$, ($v_{HE}$ is the slope of the dispersion at high binding energy and v_F is the Fermi velocity) measuring the strength of the (mostly spin-mediated) interaction, is plotted vs. x. Although our analysis was limited to $x \geqslant 0.15$, extrapolating to lower x the increasing strength of the scattering mediated by spin fluctuations (see Ref. 17), we can also account for the observed[47] increase of the parameter λ (along with the increase of v_{HE}) below $x = 0.15$.

IV. CONCLUSION

In conclusion, the salient aspects of ARPES experiments in LSCO are well reproduced by the *same* two (mixed phonon-charge and spin) collective modes previously obtained to fit Raman experiments. This finding provides further support to the increasingly widespread idea that two collective modes mediate the relevant interactions in cuprates.[17–19] In this perspective, our results provide a natural answer, at least for LSCO, to the long-standing issue whether the kinks are due to phonons or spin fluctuations: We reach the Solomonic conclusion that both play a role. By the interplay of the two collective modes, we can also explain the highly nontrivial doping evolution of the low- and high-energy quasiparticle velocity along the nodal (ΓX) direction, with v_F almost doping independent and v_{HE} decreasing with increasing doping, along with the suppression of the coupling with the spin collective mode.

The charge-spin cooperative behavior might be specific of LSCO, where the tendency to charge ordering seems to be more pronounced than, e.g., in YBCO, where the kinks are more rounded. However, recent experiments[15,16] pinpointed strong signatures of charge ordering also for YBCO. We also point out that our analysis only holds above T_c. Below T_c the spin collective mode changes and displays the peculiar resonance at (π,π), which alters the shape of the kinks, producing a characteristic s-shaped dispersion in the antinodal regions.[31,48] On the other hand, the rather broad and moderately coupled phonons should keep their effects (most pronounced around the nodal regions) even in the superconducting phase. We therefore expect that the mixed phonon-charge collective mode put in evidence by our analysis maintains its main characteristics at $T < T_c$.

Our analysis also predicts a kink and a low-energy rounding (analogous to those observed in BSCCO[45,46]) and additional waterfalls at high binding energy, along a square contour around the Γ point of the BZ, which call for further experimental investigation.

Our phenomenological model substantiates the presence of a charge and spin quasi-ordered phase compatible with fluctuating stripes and competing with superconductivity. The mixed phonon-charge and spin collective modes are also natural candidates for the pairing glue in cuprates.

ACKNOWLEDGMENTS

S.C., C.D.C., and M.G. acknowledge financial support from the "University Research Project" of the "Sapienza" University No. C26A115HTN.

[1] S. Caprara, C. Di Castro, S. Fratini, and M. Grilli, Phys. Rev. Lett. **88**, 147001 (2002).
[2] S. Caprara, C. Di Castro, M. Grilli, and D. Suppa, Phys. Rev. Lett. **95**, 117004 (2005).
[3] S. Caprara, M. Grilli, C. Di Castro, and T. Enss, Phys. Rev. B **75**, 140505(R) (2007).
[4] P. W. Anderson, Science **316**, 1705 (2007).
[5] T. A. Maier, D. Poilblanc, and D. J. Scalapino, Phys. Rev. Lett. **100**, 237001 (2008).
[6] W. Hanke, M. L. Kiesel, M. Aichhorn, S. Brehm, and E. Arrigoni, Eur. Phys. J. Special Topics **188**, 15 (2010).

[7]Ar. Abanov, A. Chubukov, and J. Schmalian, Adv. Phys. **52**, 119 (2003), and references therein.
[8]C. M. Varma, Phys. Rev. Lett. **75**, 898 (1995); Phys. Rev. B **55**, 14554 (1997), and references therein.
[9]L. Benfatto, S. Caprara, and C. Di Castro, Eur. Phys. J. B **17**, 95 (2000).
[10]S. Chakravarty, R. B. Laughlin, D. K. Morr, and C. Nayak, Phys. Rev. B **63**, 094503 (2001).
[11]W. Metzner, D. Rohe, and S. Andergassen, Phys. Rev. Lett. **91**, 066402 (2003).
[12]C. Castellani, C. Di Castro, and M. Grilli, Phys. Rev. Lett. **75**, 4650 (1995).
[13]U. Löw, V. J. Emery, K. Fabricius, and S. A. Kivelson, Phys. Rev. Lett. **72**, 1918 (1994).
[14]S. A. Kivelson, I. P. Bindloss, E. Fradkin, V. Oganesyan, J. M. Tranquada, A. Kapitulnik, and C. Howald, Rev. Mod. Phys. **75**, 1201 (2003), and references therein.
[15]G. Ghiringhelli *et al.*, Science Magazine **337**, 821 (2012).
[16]J. Chang, E. Blackburn, A. T. Holmes, N. B. Christensen, J. Larsen, J. Mesot, Ruixing Liang, D. A. Bonn, W. N. Hardy, A. Watenphul, M. V. Zimmermann, E. M. Forgan, and S. M. Hayden, Nat. Phys. **8**, 871 (2012).
[17]S. Caprara, C. Di Castro, B. Muschler, W. Prestel, R. Hackl, M. Lambacher, A. Erb, S. Komiya, Y. Ando, and M. Grilli, Phys. Rev. B **84**, 054508 (2011).
[18]E. van Heumen, E. Muhlethaler, A. B. Kuzmenko, H. Eisaki, W. Meevasana, M. Greven, and D. van der Marel, Phys. Rev. B **79**, 184512 (2009).
[19]S. Dal Conte, C. Giannetti, G. Coslovich, F. Cilento, D. Bossini, T. Abebaw, F. Banfi, G. Ferrini, H. Eisaki, M. Greven, A. Damascelli, D. van der Marel, and F. Parmigiani, Science **335**, 1600 (2012).
[20]C. Castellani, C. Di Castro, and M. Grilli, Z. Phys. B **103**, 137 (1997).
[21]C. Castellani, C. Di Castro, and M. Grilli, J. Phys. Chem. Solids **59**, 1694 (1998).
[22]J. L. Tallon and J. W. Loram, Physica C **349**, 53 (2001).
[23]A. Perali, C. Castellani, C. Di Castro, and M. Grilli, Phys. Rev. B **54**, 16216 (1996).
[24]S. Andergassen, S. Caprara, C. Di Castro, and M. Grilli, Phys. Rev. Lett. **87**, 056401 (2001).
[25]For a review, see, e.g., D. R. Garcia and A. Lanzara, Adv. Cond. Mat. Phys. (2010), doi: 10.1155/2010/807412, and references therein.
[26]J. Graf, G.-H. Gweon, K. McElroy, S. Y. Zhou, C. Jozwiak, E. Rotenberg, A. Bill, T. Sasagawa, H. Eisaki, S. Uchida, H. Takagi, D.-H. Lee, and A. Lanzara, Phys. Rev. Lett. **98**, 067004 (2007).
[27]J. Chang, S. Pailhés, M. Shi, M. Manson, T. Claesson, O. Tjernberg, J. Voigt, V. Perez, L. Patthey, N. Momono, M. Oda, M. Ido, A. Schnyder, C. Mudry, and J. Mesot, Phys. Rev. B **75**, 224508 (2007).
[28]X. J. Zhou, T. Cuk, T. Devereaux, N. Nagaosa, and Z.-X. Shen, *Angle-Resolved Photoemission Spectroscopy on Electronic Structure and Electron-Phonon Coupling in Cuprate Superconductors*, Handbook of High-Temperature Superconductivity: Theory and Experiment, edited by J. R. Schrieffer (Springer, New York, 2007), pp. 87–144.
[29]P. V. Bogdanov, A. Lanzara, S. A. Kellar, X. J. Zhou, E. D. Lu, W. J. Zheng, G. Gu, J.-I. Shimoyama, K. Kishio, H. Ikeda, R. Yoshizaki, Z. Hussain, and Z. X. Shen, Phys. Rev. Lett. **85**, 2581 (2000).
[30]T. Dahm, V. Hinkov, S. V. Borisenko, A. A. Kordyuk, V. B. Zabolotnyy, J. Fink, B. Bchner, D. J. Scalapino, W. Hanke, and B. Keimer, Nat. Phys. **5**, 217 (2009).
[31]A. V. Chubukov and M. R. Norman, Phys. Rev. B **70**, 174505 (2004).
[32]S. Caprara, M. Sulpizi, A. Bianconi, C. Di Castro, and M. Grilli, Phys. Rev. B **59**, 14980 (1999).
[33]A. J. Millis, H. Monien, and D. Pines, Phys. Rev. B **42**, 167 (1990).
[34]F. Becca, M. Tarquini, M. Grilli, and C. Di Castro, Phys. Rev. B **54**, 12443 (1996).
[35]K. Yamada, C. H. Lee, K. Kurahashi, J. Wada, S. Wakimoto, S. Ueki, H. Kimura, Y. Endoh, S. Hosoya, G. Shirane, R. J. Birgeneau, M. Greven, M. A. Kastner, and Y. J. Kim, Phys. Rev. B **57**, 6165 (1998).
[36]J. M. Tranquada, B. J. Sternlieb, J. D. Axe, Y. Nakamura, and S. Uchida, Nature (London) **375**, 561 (1995).
[37]P. Abbamonte, A. Rusydi, S. Smadici, G. D. Gu, G. A. Sawatzky, and D. L. Feng, Nat. Phys. **1**, 155 (2005).
[38]A. P. Kampf and J. R. Schrieffer, Phys. Rev. B **42**, 7967 (1990).
[39]M. Grilli, G. Seibold, A. Di Ciolo, and J. Lorenzana, Phys. Rev. B **79**, 125111 (2009).
[40]Susmita Basak, Tanmoy Das, Hsin Lin, J. Nieminen, M. Lindroos, R. S. Markiewicz, and A. Bansil, Phys. Rev. B **80**, 214520 (2009).
[41]R. S. Markiewicz, S. Sahrakorpi, and A. Bansil, Phys. Rev. B **76**, 174514 (2007).
[42]A. Macridin, M. Jarrell, T. Maier, and D. J. Scalapino, Phys. Rev. Lett. **99**, 237001 (2007).
[43]W. Meevasana, X. J. Zhou, S. Sahrakorpi, W. S. Lee, W. L. Yang, K. Tanaka, N. Mannella, T. Yoshida, D. H. Lu, Y. L. Chen, R. H. He, Hsin Lin, S. Komiya, Y. Ando, F. Zhou, W. X. Ti, J. W. Xiong, Z. X. Zhao, T. Sasagawa, T. Kakeshita, K. Fujita, S. Uchida, H. Eisaki, A. Fujimori, Z. Hussain, R. S. Markiewicz, A. Bansil, N. Nagaosa, J. Zaanen, T. P. Devereaux, and Z.-X. Shen, Phys. Rev. B **75**, 174506 (2007).
[44]A. V. Chubukov, D. K. Morr, and A. Shakhnovich, Philos. Mag. B **74**, 563 (1996); A. V. Chubukov and D. K. Morr, Phys. Rep. **288**, 355 (1997).
[45]I. M. Vishik, W. S. Lee, F. Schmitt, B. Moritz, T. Sasagawa, S. Uchida, K. Fujita, S. Ishida, C. Zhang, T. P. Devereaux, and Z. X. Shen, Phys. Rev. Lett. **104**, 207002 (2010).
[46]S. Johnston, I. M. Vishik, W. S. Lee, F. Schmitt, S. Uchida, K. Fujita, S. Ishida, N. Nagaosa, Z. X. Shen, and T. P. Devereaux, Phys. Rev. Lett. **108**, 166404 (2012).
[47]S. Sahrakorpi, R. S. Markiewicz, Hsin Lin, M. Lindroos, X. J. Zhou, T. Yoshida, W. L. Yang, T. Kakeshita, H. Eisaki, S. Uchida, Seiki Komiya, Yoichi Ando, F. Zhou, Z. X. Zhao, T. Sasagawa, A. Fujimori, Z. Hussain, Z.-X. Shen, and A. Bansil, Phys. Rev. B **78**, 104513 (2008).
[48]U. Chatterjee, D. K. Morr, M. R. Norman, M. Randeria, A. Kanigel, M. Shi, E. Rossi, A. Kaminski, H. M. Fretwell, S. Rosenkranz, K. Kadowaki, and J. C. Campuzano, Phys. Rev. B **75**, 172504 (2007).